

Free Electron Laser Seeded by ir Laser Driven High-order Harmonic Generation *

Juhao Wu,^{1,†} Paul R. Bolton,¹ James B. Murphy,² and Xinming Zhong³

¹Stanford Linear Accelerator Center, Stanford University, Stanford, CA 94309

²National Synchrotron Light Source, Brookhaven National Laboratory, Upton, NY 11973-5000

³Institute of Low Energy Nuclear Physics, Beijing Normal University, Beijing 100875, P. R. China
(Dated: June 06, 2006)

Coherent x-ray production by a seeded free electron laser (FEL) is important for next generation synchrotron light sources. We examine the feasibility and features of FEL emission seeded by a high-order harmonic of an infrared laser (HHG). In addition to the intrinsic FEL chirp, the longitudinal profile and spectral bandwidth of the HHG seed are modified significantly by the FEL interaction well before saturation. This smears out the original attosecond pulselet structure. We introduce criteria for this smearing effect on the pulselet and the stretching effect on the entire pulse. We discuss the noise issue in such a seeded FEL.

Short-wavelength Free-electron Lasers (FELs) are considered to be the next generation of synchrotron light sources. The dominant scheme for the x-ray FEL (XFEL) is Self-Amplified Spontaneous Emission (SASE) [1–4]. Due to a short longitudinal coherent length, SASE FEL pulse consists of a series of ultrashort spikes, and is therefore longitudinally incoherent, yet it has good transverse coherence. Cascaded high gain harmonic generation (HG) [5–9], seeded by high-order harmonic generation (HHG) from an infrared (ir) laser source shows promise for improving the longitudinal coherence [10, 11]. HHG can provide a seed ranging from the uv to the soft x-ray region, making it feasible to consider longitudinal and transverse coherent XFEL in the hard x-ray region.

The HHG electric field consists of multiple orders, s with wavenumber, k_s and angular frequency, ω_s , and multiple pulselets, n as a double summation:

$$E_{\text{HHG}}(t, z) = \sum_s E_{s,0} e^{i(k_s z - \omega_s t)} e^{-i\mathcal{B}_s \omega_s^2 t^2} \times \sum_{n=-N}^N e^{-\frac{t_n^2}{4\sigma_{t,0}^2}} e^{-\alpha_s \omega_s^2 [(t-t_n) - z/c]^2}, \quad (1)$$

where $E_{s,0}$ is the peak amplitude of the electric field. For each order, the temporal structure is a sequence of $2N+1$ ultrashort pulselets with attosecond structure which is referred as the attosecond pulse train (APT). Pulselet peaks occur at times, $t_n = n\tau/2$ where τ is the ir laser period. With multiple orders the duration of a single attosecond pulselet (SAP) is significantly less than one femtosecond and limited by the relative amplitudes and spectral phases of the different orders [12]. The temporal envelope of the entire HHG pulse has an rms duration

$\sigma_{t,0}$. We define the much shorter rms duration, $\sigma_{t,s}$ for the single attosecond pulselet duration for harmonic order, s with $\alpha_s \omega_s^2 \equiv 1/(4\sigma_{t,s}^2)$. The single harmonic seed chirp [13], $\mathcal{B}_s \approx -\frac{\mathcal{A}_s I_{ir}}{2(s\omega_{ir}\sigma_{t,ir})^2} + \frac{b_{ir}}{2s\omega_{ir}^2}$ has two terms. The first term is an intrinsic order-dependent dipole contribution that scales linearly with some coefficient, \mathcal{A}_s , but also depends on the ir laser intensity, I_{ir} laser frequency, ω_{ir} and laser pulse rms duration, $\sigma_{t,ir}$. The second term is inherited from the chirp, b_{ir} of the ir laser waveform. We neglect the well-known positive chirp of multiple order emission that is attributed to the spectral phase delay of the different orders as well as contributions from time-dependent alterations to the refractive index of the gaseous conversion medium (*e.g.*, ionization effects).

We consider an HHG seed with central frequency (carrier) being only a single harmonic order, s . For simplicity, we neglect the chirp \mathcal{B}_s . The HHG seed field reduces to:

$$E_s(t, z) = E_{s,0} e^{i(k_s z - \omega_s t)} \sum_{n=-N}^N e^{-\frac{t_n^2}{4\sigma_{t,0}^2}} \times e^{-\alpha_s \omega_s^2 [(t-t_n) - z/c]^2}. \quad (2)$$

This APT is simply the amplitude modulation of a single carrier frequency, ω_s . We use $\sigma_{t,0} = 10$ fsec, $\sigma_{t,s} = \tau/10 \approx 267$ attoseconds in the Fourier transform limit, and the ir laser wavelength $\lambda_{ir} = 800$ nm in this letter.

To illustrate the derivation, we focus on a single pulselet of Eq. (2) for which $n = 0$ and $t_n = 0$ and $E_s(t, z = 0) = E_{s,0} \exp(-i\omega_s t - \alpha_s \omega_s^2 t^2)$. In the transform limit, $\sigma_{t,s} \sigma_{\omega,s} = 1/2$ and the rms pulselet bandwidth, $\sigma_{\omega,s} = \omega_s \sqrt{\alpha_s}$. The seeded FEL is: [14, 15]

$$E_{\text{FEL}}(t, z) = E_{0,\text{FEL}} e^{\rho(\sqrt{3}+i)k_w z} \times e^{i(k_s z - \omega_s t)} e^{-[\alpha_{s,f}(z) + i\beta_{s,f}(z)]\omega_s^2 (t-z/v_g)^2}, \quad (3)$$

where $v_g = \omega_s / (k_s + 2/3k_w)$ is the group velocity of the FEL light. In Eq. (3), $\alpha_{s,f}(z) = [4\sigma_{t,s,f}^2(z)\omega_s^2]^{-1}$ and

*The work of JW and PRB was supported by the US Department of Energy under contract DE-AC02-76SF00515. The work of JBM was supported by the US Department of Energy under contract DE-AC02-98CH10886 and the Office of Naval Research.

†Electronic address: jhwu@SLAC.Stanford.EDU

$\beta_{s,f}^2(z) = \alpha_{s,f}(z)\sigma_{\omega,s,f}^2(z)/\omega_s^2 - \alpha_{s,f}^2(z)$, with

$$\begin{cases} \sigma_{t,s,f}(z) = \sigma_{t,s}\sqrt{1+R(z)^2+R(z)^4/\{3[1+R(z)^2]\}} \\ \sigma_{\omega,s,f}(z) = \sigma_{\omega,s}/\sqrt{1+R(z)^2} \end{cases}, \quad (4)$$

$$R(z) \equiv \sigma_{\omega,s}/\sigma_{\omega,\text{GF}}(z), \quad \sigma_{\omega,\text{GF}}(z) \equiv \sqrt{3\sqrt{3}\rho\omega_s^2/(k_w z)}. \quad (5)$$

Here $\sigma_{\omega,\text{GF}}(z)$ is the rms bandwidth of the FEL Green function for a coasting electron beam with the Pierce parameter [1], $\rho = 1/(2\gamma_0)\{4K^2[JJ]^2/(k_w^2 R_0^2)I_{pk}/I_A\}^{1/3}$ where $\gamma_0 = \sqrt{(1+K^2/2)\lambda_w/(2\lambda_s)}$ is the Lorentz factor of the electron resonant energy with λ_s the s^{th} order HHG seed wavelength; $K \approx 93.4B_w\lambda_w$ where B_w is the undulator peak field in Teslas and period λ_w in meters; $[JJ] = J_0[\frac{a_w^2}{2(1+a_w^2)}] - J_1[\frac{a_w^2}{2(1+a_w^2)}]$, with $a_w = K/\sqrt{2}$, J_0 and J_1 being the 0th-order and 1st-order Bessel functions; $k_w = 2\pi/\lambda_w$; R_0 is the electron beam hard edge; I_{pk} is the peak current; and $I_A \equiv 4\pi\epsilon_0 mc^3/e \approx 17045$ Amp, the Alfvén current. For a unchirped seed $\alpha_{s,f}(0) = \alpha_s$, $\beta_{s,f}(0) = \beta_s = 0$, $\sigma_{t,s,f}(0) = \sigma_{t,s}$, and $\sigma_{\omega,s,f}(0) = \sigma_{\omega,s}$. The FEL-interaction intrinsically generates a chirped FEL, $\langle(t - \langle t \rangle)(\omega - \langle \omega \rangle)\rangle = \frac{\beta_{s,f}(z)}{2\alpha_{s,f}(z)} = \frac{R(z)^2}{2\sqrt{3[1+R(z)^2]}}$. The emittance of the FEL light at any position, z , is conserved, $\varepsilon \equiv \{ \langle(t - \langle t \rangle)^2\rangle\langle(\omega - \langle \omega \rangle)^2\rangle - \langle(t - \langle t \rangle)(\omega - \langle \omega \rangle)\rangle^2 \}^{1/2} = 1/2$, indicating a fully longitudinally coherent FEL [14]. For adequately large z , $R(z) \gg 1$ and the FEL emission is characterized as: $\sigma_{t,s,f}(z) \rightarrow [\sqrt{3}\sigma_{\omega,\text{GF}}(z)]^{-1}$, $\sigma_{\omega,s,f}(z) \rightarrow \sigma_{\omega,\text{GF}}(z)$, and $\langle(t - \langle t \rangle)(\omega - \langle \omega \rangle)\rangle \rightarrow (2\sqrt{3})^{-1}$. As in Eq. (4), the FEL interaction can significantly reduce an initially broadband seed within a short distance, thereby extending its temporal duration and smearing out attosecond structure.

We have defined a critical location, z_c within the undulator ($z = 0$ as the entrance plane) where the FEL Green function bandwidth is reduced to the incident seed pulselet bandwidth, *i.e.*, $R(z_c) = 1$ [11] when we take $\sigma_{\omega,s} = (\sigma_{\omega,s})_{\text{pulselet}}$. If the incident seed pulselet bandwidth ratio, $(\sigma_{\omega,s}/\omega_s)_{\text{pulselet}}$ exceeds the critical bandwidth ratio, $(\sigma_{\omega,s}/\omega_s)_c$, where $(\sigma_{\omega,s}/\omega_s)_c \equiv 3\sqrt{2}\rho$, then z_c is less than the power gain length, $L_G \equiv \lambda_w/(4\pi\sqrt{3}\rho)$.

In this letter, we address a simple generic FEL amplifier using a linac coherent light source (LCLS)-type undulator [16] with $\lambda_w = 3$ cm and undulator parameter $K = 3.5$. For 30 nm HHG seed, *i.e.*, the 27th harmonic, we scale the LCLS-type electron beam parameters according to the resonance condition. The system has $\rho = 6.3 \times 10^{-3}$, so $L_G = 0.22$ m. For these parameters, $z_c = 0.18$ m. Hence, the attosecond pulselet structure is smeared out quickly as in Fig. 1 (a). Assuming a seed power of $P_s = 5$ MW [17], saturation happens at $L_{\text{sat}} = 4.2$ m with a power of 12 GW.

With this example it is important to note that, although we consider only a single order carrier frequency, for adequately short $\sigma_{t,s}$ ($\sigma_{t,s} = \tau/10$ here), the transform limited seed spectrum can include components from

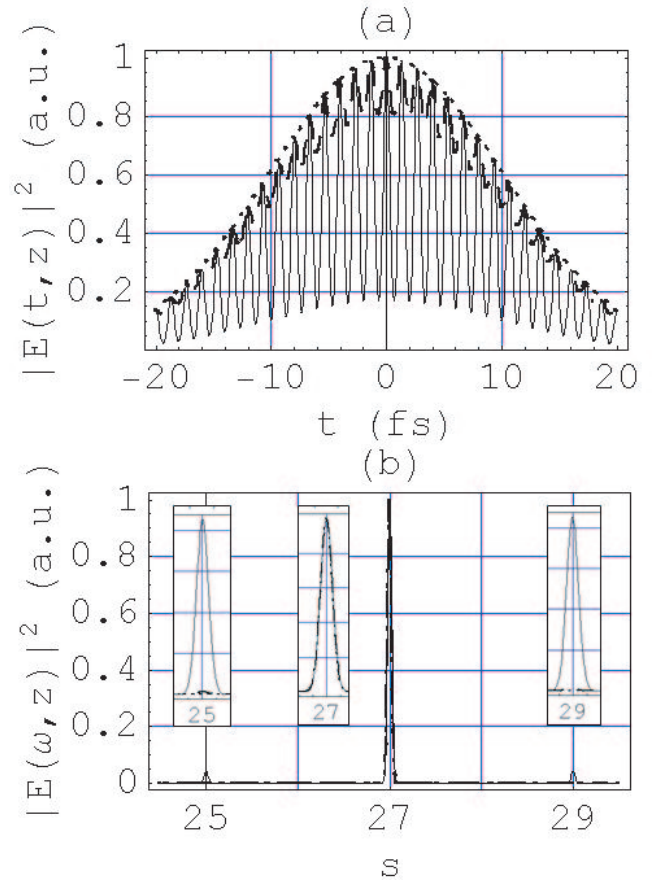


FIG. 1: (a) Illustration of smearing effect of the attosecond pulselet. The solid curve is at $z = 0$, the dashed curve at $z = z_c = 0.18$ m, and the dotted curve at $z = L_{\text{sat}} = 4.2$ m. (b) FEL intensity spectrum as a function of harmonic number, s . The insets show a blowup near the 25th, 27th, and 29th harmonics. Notations are the same as in (a).

neighboring harmonic orders. In Fig. 1 (b), the spectrum components of the 25th and 29th harmonics are seen clearly in the initial seed. However, as shown in Fig. 1 (b), these components disappear quickly. To better characterize this spectrum narrowing behavior, we introduce a second critical location, z_s where the FEL Green function FWHM bandwidth reduces to that of the nearest neighboring harmonic, *i.e.*, $\sqrt{2\ln(2)}\sigma_{\omega,\text{GF}}(z_s)/\omega_s = 2/s$. For the above example, $z_s = 0.04$ m. The smallness of z_s guarantees that the simplification from Eq. (1) to Eq. (2) is an extremely good approximation, *i.e.*, the FEL acts like a narrow bandwidth filter so that the adjacent harmonics are essentially irrelevant.

In addition we define a third critical location, z_e for which the FEL Green function bandwidth is reduced to that attributed only to the longer temporal envelop of the entire HHG seed pulse, *i.e.*, $\sigma_{\omega,\text{GF}}(z_e) = (\sigma_{\omega,s})_{\text{pulse}} = 1/(2\sigma_{t,0})$ for a transform limit seed. Notice that $R(z_e) \gg 1$, and $(\sigma_{\omega,s})_{\text{pulse}} \ll (\sigma_{\omega,s})_{\text{pulselet}}$ at $z = 0$, hence z_e is large enough for any attosecond pulselet structure to have been lost. If the bandwidth of the

entire pulse, $(\sigma_{\omega,s})_{\text{pulse}}$ is narrower than a critical ratio of $(\sigma_{\omega,s})_e \equiv \rho\omega_s\sqrt{3\sqrt{3}/(2\pi f)} = 3\rho\omega_s\sqrt{2L_G/L_{\text{sat}}}$, then $z_e > L_{\text{sat}}$ where $L_{\text{sat}} \equiv f\lambda_w/\rho$ is the seeded FEL saturation length. Notice that L_{sat} is a fraction f of the SASE FEL saturation length, *i.e.*, $f = 1$ for SASE. For the above example, $f \approx 0.9$. Shown in Fig. 1 (b), the numerically obtained rms bandwidth of the 27th harmonic is almost $1/(2\sigma_{t,0})$, which is the rms bandwidth determined by the pulse envelope. For the above example, $z_e \approx 253$ m. Since $z_e \gg L_{\text{sat}}$, there is no bandwidth reduction on the entire pulse, hence no pulse stretching.

As a summary, we require $z_s \ll z_c < L_G$ to ensure Eq. (2), *i.e.*, taking only the resonant frequency, being a good approximation. We require $z_c < L_G$ to render the HHG seed pulse similar in effect to a typical harmonic seed generated by wave mixing in an anisotropic crystal, *i.e.*, lacking the attosecond pulselet structure. Furthermore, to eliminate temporal broadening of the entire HHG pulse envelope, we also need $z_e > L_{\text{sat}}$. The combination of the latter two conditions means that $z_e/z_c > L_{\text{sat}}/L_G$ and $[(\sigma_{\omega,s})_{\text{pulselet}}/(\sigma_{\omega,s})_{\text{pulse}}]^2 > L_{\text{sat}}/L_G$. The latter two conditions also suggest a constraint on the incident HHG seed pulse temporal structure, *i.e.* a comparison of the longer temporal envelope and the much shorter pulselet structure. In the transform limit, the $z_c < L_G$ condition requires that for seed harmonic order, s the pulselet timescale, $\sigma_{t,s} < 1/(6\sqrt{2}\rho s\omega_{ir})$. The $z_e > L_{\text{sat}}$ condition requires that the longer pulse timescale, $\sigma_{t,0} > \sqrt{\pi f/(6\sqrt{3})}/(\rho s\omega_{ir})$. So, for $t \in [-\sigma_{t,0}, \sigma_{t,0}]$, the minimum pulselets number, m_l that an HHG seed pulse must contain is about: $m_l \approx 1 + \frac{4\sigma_{t,0}}{\tau} \geq 1 + \frac{4}{\omega_{ir}\tau\rho s} \sqrt{\frac{\pi f}{6\sqrt{3}}}$. With $\omega_{ir}\tau = 2\pi$, $m_l > 3$, and $\sigma_{t,0} > 1.3$ fsec for the above example. Increasing the Pierce parameter or the harmonic order reduces the $\sigma_{t,0}$ minimum and therefore the required minimum pulselets number, m_l .

Undulator radiation and SASE FEL always exist as noise [18] in a seeded FEL. The effective start-up noise power for the fundamental SASE guiding mode is [9, 19]

$$P_{\text{SASE}}^{\text{Start-up}} = C_1 (2L_G/L_w) \pi(2\lambda_s/L_w) \sqrt{3\sqrt{3}\rho/N_w} \times \frac{eZ_0 I_{pk} N_w^2 \gamma^2 K^2}{4\pi (1 + K^2/2)^2} [JJ]^2 \omega_s, \quad (6)$$

where the coupling factor is found to be [19], $C_m(a) \approx \frac{\sqrt{3}}{\pi a^2} \exp[-\frac{1}{a\sqrt{1+a^2}}(\beta_{m,0} + \beta_{m,1}\frac{1}{a^2})]$ for $a > 0.25$, where, m is the index referring to the m^{th} mode excitation; $a = \sqrt{4\rho k_w k_s} R_0$ is the scaled beam size. For the fundamental guiding mode ($m = 1$), $\beta_{1,0} = 1.093$, and $\beta_{1,1} = -0.02$. In Eq. (6), $N_w (= L_w/\lambda_w)$ is the undulator period number with L_w the undulator length; Z_0 is the vacuum impedance. In the above SASE calculation, at $z = 2L_G$ the bandwidth of the fundamental guided mode is $\sigma_{\omega,\text{GF}}(z = 2L_G)$ according to Eq. (5). But, the seeded FEL has a different bandwidth of $\sigma_{\omega,s,f}(z = 2L_G)$ according to Eq. (4). Hence, the true start-up noise power within the seeded FEL bandwidth is estimated as

$$P_{\text{Seeded}}^{\text{Start-up}} = P_{\text{SASE}}^{\text{Start-up}} [\sigma_{\omega,s,f}(z)/\sigma_{\omega,\text{GF}}(z)]|_{z=2L_G}. \quad (7)$$

Considering the above mentioned case with $L_w \approx L_{\text{sat}}$ and $I_{pk} = 3.4$ kA, we have $a \approx 2.2$, so that $C_1 \approx 0.09$. According to Eq. (6), the SASE effective start-up noise power in the fundamental guided mode is $P_{\text{SASE}}^{\text{Start-up}} \approx 60$ W. We consider the plane, $z = 2L_G$ where the attosecond structure is lost ($z_c \ll 2L_G$) and the relevant seed bandwidth ratio $\sigma_{\omega,s,f}/\omega_s$ is the pulse bandwidth ratio. For $\sigma_{t,0} = 10$ fsec in the transform limit, this ratio is about twenty four times smaller than the SASE bandwidth ratio of 1.9 %. The true start-up noise power is reduced from 60 W to 2.5 W. For a cascaded FEL scheme (HGFG), we estimate the seed power P_s level required to generate XFEL radiation with good longitudinal coherence of wavelength, λ_r in terms of the noise-to-signal (NTS) ratio. For HGFG, the NTS ratio amplification scales as n_h^2 with $n_h = \lambda_s/\lambda_r = (\lambda_{ir}/\lambda_r)/s$ [9, 18]. Hence, the final XFEL NTS is $\text{NTS}_r = n_h^2 (P_{\text{Seeded}}^{\text{Start-up}}/P_s) = [(\lambda_{ir}/\lambda_r)/s]^2 P_{\text{Seeded}}^{\text{Start-up}}/P_s$. So, $\text{NTS}_r \leq 0.1$ requires that $P_s \geq 2.25$ MW for $\lambda_r = 0.1$ nm, and $s = 27$ with $P_{\text{Seeded}}^{\text{Start-up}} = 2.5$ W. Obtaining 2.25 MW seed power may need various harmonic power enhancement schemes [20, 21]. Furthermore as shown in Eqs. (6) and (7), the true startup noise power depends on various FEL parameters. With more detailed simulation, these parameters can be separately optimized to reduce NTS within the constraint of preserving the exponential FEL power gain.

[1] R. Bonifacio, C. Pellegrini, and L.M. Narducci, Opt. Commun., **50**, 373 (1984).
[2] J.-M. Wang and L.-H. Yu, Nucl. Instr. and Meth., **A 250**, 484 (1986).
[3] K.-J. Kim, *ibid.*, **A 250**, 396 (1986); Phys. Rev. Lett. **57**, 1871 (1986); Lawrence Berkeley National Laboratory Report No. 40672 (1997).
[4] S. Krinsky and Z. Huang, Phys. Rev. ST Accel. Beams **6**, 050702 (2003); E.L. Saldin, E.A. Schneidmiller, and M.V. Yurkov, *ibid.* **9**, 050702 (2006).
[5] L.H. Yu, Phys. Rev. A **44**, 5178(1991).

[6] J. Wu and L.H. Yu, Nucl. Instr. and Meth., **A 475**, 104 (2001).
[7] L.H. Yu and J. Wu, *ibid.*, **A 483**, 493 (2002).
[8] J. Wu and L.H. Yu, Stanford Linear Accelerator Center Report No. SLAC-PUB-10494 (2004).
[9] J. Wu and L.H. Yu, SLAC-PUB-10495 (2004).
[10] M.-E. Couprie *et al.*, Proc., 2005 Int. FEL Conf., p.55.
[11] J. Wu and P.R. Bolton, SLAC-PUB-12124 (2006).
[12] R. López-Martens *et al.*, Phys. Rev. Lett. **94**, 033001 (2005).
[13] J. Mauritsson *et al.*, Phys. Rev. A **70**, 021801(R) (2004).

- [14] J.B. Murphy, J. Wu, X.J. Wang, and T. Watanabe, Brookhaven National Laboratory Report BNL-75807-2006-JA, and SLAC-PUB-11852 (2006).
- [15] J. Wu, J.B. Murphy, P.J. Emma, X.J. Wang, T. Watanabe, and X. Zhong, *J. Opt. Soc. Am. B* **24**, 484 (2007).
- [16] J. Arthur *et al.*, SLAC-R-593 (2002).
- [17] E. Takahashi, Y. Nabekawa, T. Otsuka, M. Obara, and K. Midorikawa, *Phys. Rev. A* **66**, 021802(R)(2002).
- [18] E.L. Saldin, E.A. Schneidmiller, and M.V. Yurkov, *Opt. Commun.* **202**, 169 (2002).
- [19] L.H. Yu, *Phys. Rev. E* **58**, 4991(1998).
- [20] A. Paul *et al.*, *Nature* **421**, 51(2003).
- [21] K.J. Schafer, M.B. Gaarde, A. Heinrich, J. Biegert, and U. Keller, *Phys. Rev. Lett.* **92**, 023003(2004).